Institute of Space and Aeronautical Science, University of Tokyo
Report No. 514, July 1974

An Envelope of a Correlation Function and its Application to a Delay Time Measurement

By

Nobuharu AOSHIMA

Summary: A new method of correlation measurement using FFT algorism is proposed. An envelope of a correlation function (or an inverse Fourier transform of a transfer function) is shown to be calculated easily by this method. Correlation envelopes are useful in measuring wave propagation, especially in dispersive wave cases. Experiments of sound propagation and flexural wave propagation are described.

1. INTRODUCTION

From an input and an output signal of a linear system, we can compute a transfer function $G(\omega)$. $G(\omega)$ is a complex-valued function of ω and if the system consists of pure delay, it is equal to $e^{-i\omega\tau}$ and represents circle in the complex (Gaussian) plane. Its real and imaginary part are both sinusoidal and its angle decreases linearly with ω. From the derivative $d\{\angle G(\omega)\}/d\omega$, we can obtain the delay time τ. If there are more than two delays, it is not simple as above. $G(\omega)$ describes complex locus in the Gaussian plane and the angle does not change with constant angular velocity. To separate many delays, it is necessary to expand $G(\omega)$ in a form $\sum_j k_j e^{-i\omega\tau_j}$. Correlation methods are useful to obtain the parameters k_j and τ_j in this expression, and it is the object of this paper to show that if we handle things in frequency domain and go back to τ-domain, useful techniques can be applied and the correlation measurements become more useful.

2. THEORY

A linear system as Fig. 1 is considered. $X(\omega)$ and $Y(\omega)$ are the Fourier transform of x(t) and y(t) respectively. If external noise does not enter, G(ω) is obtained as $G(\omega)=Y(\omega)/X(\omega)=X^*(\omega)\cdot Y(\omega)/X^*(\omega)\cdot X(\omega)$, where $*$ means complex conjugate. If noise comes as Fig. 1(b), then $G'(\omega)=Y(\omega)/X(\omega)=G(\omega)+N(\omega)/X(\omega)$. External noise n(t) is assumed to be zero mean random signal and independent with x(t). Then $G(\omega)$ is obtained by taking average of $G'(\omega)$. This is the same thing as to compute $G(\omega)$ from the cross-spectrum $E[X^*\cdot Y]$ and the power spectrum $E[X^*\cdot X]$, assuming the averaging and the dividing can be interchanged. $E[\ ]$ means to take an ensemble average.

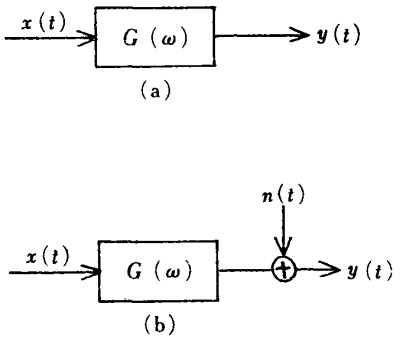

FIG. 1. A linear system considered.

Now, from the transfer function $G(\omega)$ thus obtained, an inpulse response $g(t)$ is computed as an inverse Fourier transform of $G(\omega)$. If the input signal is a white noise, $g(t)$ is equal to the cross-correlation of the input and the output signal. On the other hand, the inverse Fourier transform of the cross-spectrum $\boldsymbol{E}[X^* \cdot Y]$ is the cross-correlation function of the actual input and output signal. By using $G(\omega)$ instead of $\boldsymbol{E}[X^* \cdot Y]$, the effect of the input spectral form is eliminated.

Further, if $G_\Delta(\omega)$ defined as follows is used,

$$G_\Delta(\omega)=\begin{cases} G(\omega) & \omega_1 \leqq \omega \leqq \omega_2 \\ 0 & \omega < \omega_1, \quad \omega_2 < \omega \end{cases} \tag{1}$$

its inverse Fourier transform $g_\Delta(\tau)$ is equal to the cross-correlation when an idea band limited noise in $\omega_1 \leqq \omega \leqq \omega_2$ is used.

In practice of correlation measurements, oscillating correlation curves are frequently obtained, and it is important to note that the delay time which corresponds to the wave propagation is the maximum of the correlation envelope, not the maximum of the correlation curve itself [*1*]. Hilbert transform of the correlation function is necessary to compute correlation envelope rigorously [*2*],[*3*]. Hilbert transform is defined as

$$\hat{f}(y)=\frac{1}{\pi}\int_{-\infty}^{\infty}\frac{f(x)}{x-y}dx \tag{2}$$

The integral is the Cauchy principal value and its computation is not easy. But if we use next relation,

$$\int_{-\infty}^{\infty}\hat{g}_\Delta(\tau)e^{-i\omega\tau}d\tau=\int_{-\infty}^{\infty}d\tau\frac{1}{\pi}\int_{-\infty}^{\infty}\frac{g_\Delta(\xi)}{\xi-\tau}d\xi e^{-i\omega\tau}=-\int_{-\infty}^{\infty}g_\Delta(\xi)\widehat{e^{-i\omega\xi}}d\xi$$

$$=\left.\begin{cases} \int_{-\infty}^{\infty}g_\Delta(\xi)ie^{-i\omega\xi}d\xi=iG_\Delta(\omega) & (\omega>0) \\ 0 & (\omega=0) \\ -\int_{-\infty}^{\infty}g_\Delta(\xi)ie^{-i\omega\xi}d\xi=-iG_\Delta(\omega) & (\omega<0) \end{cases}\right\}=L_\Delta(\omega) \tag{3}$$

the Hilbert transform of $g_\Delta(\tau)$ is obtained as the inverse Fourier transform of $L_\Delta(\omega)$.

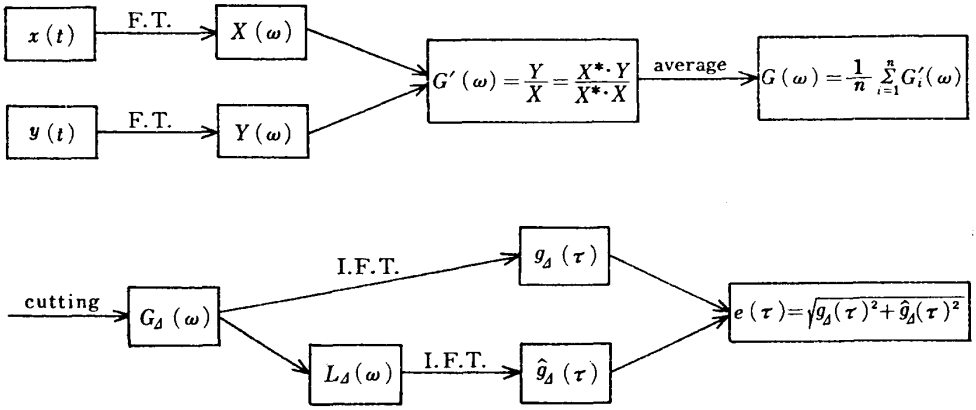

FIG. 2. A block diagram of the signal processing. F.T. means the Fourier transform and I.F.T. means the inverse Fourier transform.

$L_\Delta(\omega)$ is obtained by just changing the real and the imaginary part of $G_\Delta(\omega)$ and the sign. Then the envelope of $g_\Delta(\tau)$ is obtained as $e(\tau)=\{g_\Delta^2(\tau)+\hat{g}_\Delta^2(\tau)\}^{1/2}$. By this method, an envelope of any wave form can be obtained from its Fourier transform. Now it is shown that by the processing of Fig. 2, the envelope of the correlation of virtual ideal noise can be computed.

Fast Fourier Transform (FFT) by digital computer would be necessary for this processing. It is useful to note next properties. One thing is that though the results do not depend on the spectral form of the input signal, $G(\omega)$ cannot be computed in the range where the power spectrum of the input signal does not exist.

Another thing is that $G_\Delta(\omega)$ can be shifted on the ω-axis without any change of the correlation envelope $e(\tau)$. To show this, a correlation function $\phi(\tau)$ and its Fourier transform $\Phi(\omega)$ are considered. Writing the Hilbert transform of $\phi(\tau)$ as $\hat{\phi}(\tau)$, next relation is derived.

$$\phi(\tau)+i\hat{\phi}(\tau)=\frac{1}{\pi}\int_{-\infty}^{0}\Phi(\omega)e^{i\omega\tau}d\omega \qquad (4)$$

Now shifted power spectrum $\Phi_s(\omega)$ (as shown in Fig. 3) is considered. Writing its inverse Fourier transform as $\phi_s(\tau)$, next relations can be proved.

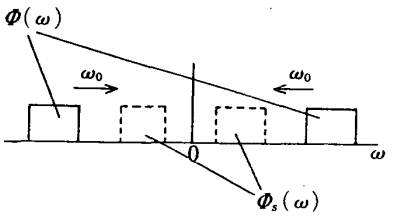

FIG. 3. Shift of a spectrum along the ω-axis. $\Phi(\omega)$ is shifted to $\Phi_s(\omega)$.

$$\phi_s(\tau)+i\hat{\phi}_s(\tau)=\frac{1}{\pi}\int_{-\infty}^{0}\Phi_s(\omega)e^{i\omega\tau}d\omega=e^{-i\omega_0\tau}\{\phi(\tau)+i\hat{\phi}(\tau)\} \qquad (5)$$

$$\therefore\quad |\phi_s(\tau)+i\hat{\phi}_s(\tau)|=|\phi(\tau)+i\hat{\phi}(\tau)| \qquad (6)$$

This means the envelope of $\phi_s(\tau)$ is equal to the envelope of $\phi(\tau)$. These propeties can be used in computer programming.

3. Experiments

(1) Sound Propagation in an Anechoic Room

Two microphones and a reflecting board are placed in an anechoic room as Fig. 4. Sound of clapping hands near the microphone 1 is used as a test signal. Signals from microphone 1 and 2 are supplied to 2 channel A-D converter and stored in core memory of a mini-computer. Then Fourier transform is made by FFT algorism and $G'(\omega)$ is calculated and stored. This process is repeated 25 times and the averaged value $G(\omega)$ is obtained. The power spectra $E[X^* \cdot X]$, $E[Y^* \cdot Y]$ and the cross-spectrum $E[X^* \cdot Y]$ are also calculated. In Fig. 5, $E[X^* \cdot X]$, $E[Y^* \cdot Y]$ and $|G(\omega)|$ are illustrated. The real and the imaginary parts of the cross-spectrum $E[X^* \cdot Y]$ are shown in Fig. 6, whose inverse Fourier transform is shown in Fig. 7(a). The upper curve is shown in full range and the lower is the magnified curve in τ-axis.

Fig. 7(a) is the same as might be obtained by ordinary correlation of x(t) and y(t), and from this figure, the delay times corresponding to the direct and the reflected sound can be determined. But in this figure, second correlation peak is not easy to determine, for the positive and the negative peak height are nearly equal. Fig. 7(b) is the envelope of (a), from which the correlation peaks can be determined easily.

In Fig. 8, the real and the imaginary part of $G(\omega)$ are shown and its inverse Fourier transform is shown in Fig. 9(a) and (b), the "correlation" curve and its envelope respectively. Comparing Fig. 7 and 9, the correlation peaks become slightly sharper by using $G(\omega)$ instead of $E[X^* \cdot Y]$, but the improvement is not much. The delay times obtained are good agreement with the calculated values from geometrical configulation.

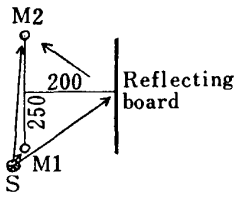

Fig. 4. The experimental setup of the microphone M1 and M2 and the reflecting board. Sound of clapping hands near M1 is used as a test signal. The output signal of M1 and M2 serve as $x(t)$ and $y(t)$.

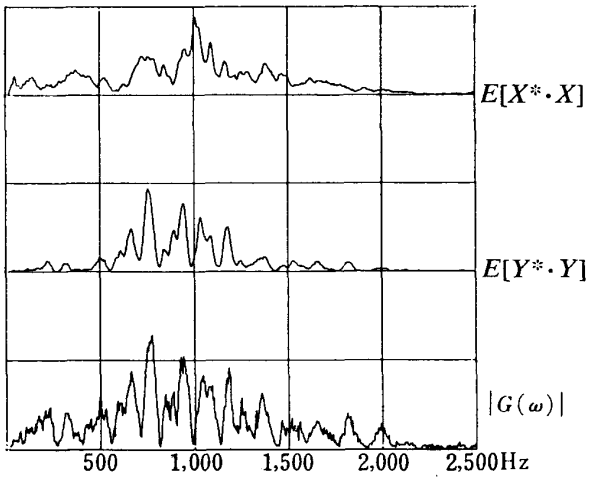

Fig. 5. The power spectra of clapping sounds $E[X^* \cdot X]$, $E[Y^* \cdot Y]$ and the magnitude of the transfer function $|G(\omega)|$ measured by FFT. The sampling period of the A-D converter is 0.2 ms.

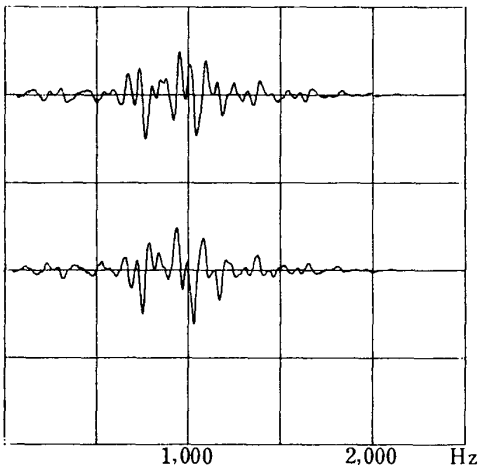

FIG. 6. The real and the imaginary part of the cross-spectrum $E[X^* \cdot Y]$.

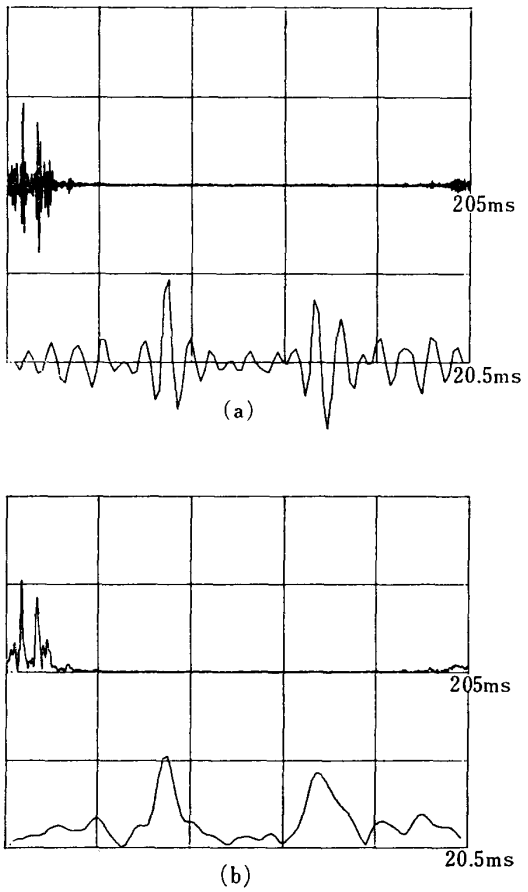

FIG. 7. (a) The inverse Fourier transform of the cross-spctrum. The lower figure is the magnified curve of one tenth of the most left part of the upper figure. The full scale of the upper figure is 205 ms, while that of the lower is 20.5 ms.
(b) The envelope of (a).

(2) Flexural Wave Propagation in a Steel Strip

A 5 m long steel strip whose cross section is 0.75×38.2^{mm} is suspended by cotton string horizontaly. Light weight (about 1 g) accelerometers are attached at 2 m and 3 m from the end and used to measure flexural wave propagation along the strip. A small metal bar (about the size of pencil) is used to strike the strip at the end to excite flexural wave. In this example, both signals from accelerometers are the mixture of direct and reflected waves, because free ends reflect flexural wave completely and an attenuation along the strip is small. So it is not suitable to regard one signal as an input and the other as an output of a system. In this situation, $E[X^* \cdot Y]$ should be analysed instead of $G(\omega)$. This is made by omitting the dividing procedure by $E[X^* \cdot X]$ in the process of Fig. 2.

The power spectra $E[X^* \cdot X]$ and $E[Y^* \cdot Y]$ are shown in Fig. 10. There are much power components above 2 kHz, but they are found little to contribute correlation peaks, so low pass filtered signals are used to analyse. Curves in Fig. 10

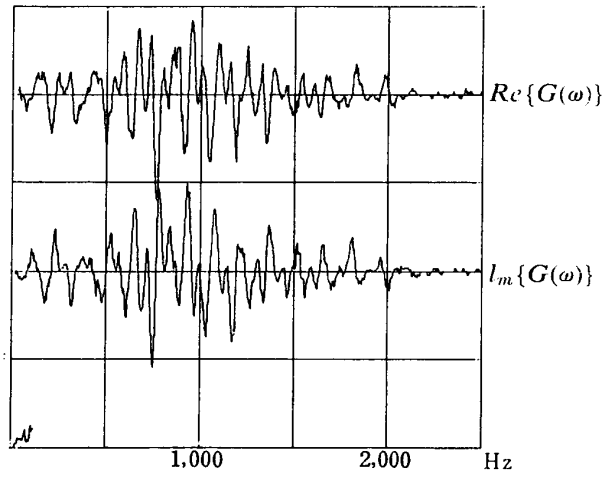

FIG. 8. The real and the imaginary part of the transfer function $G(\omega)$.

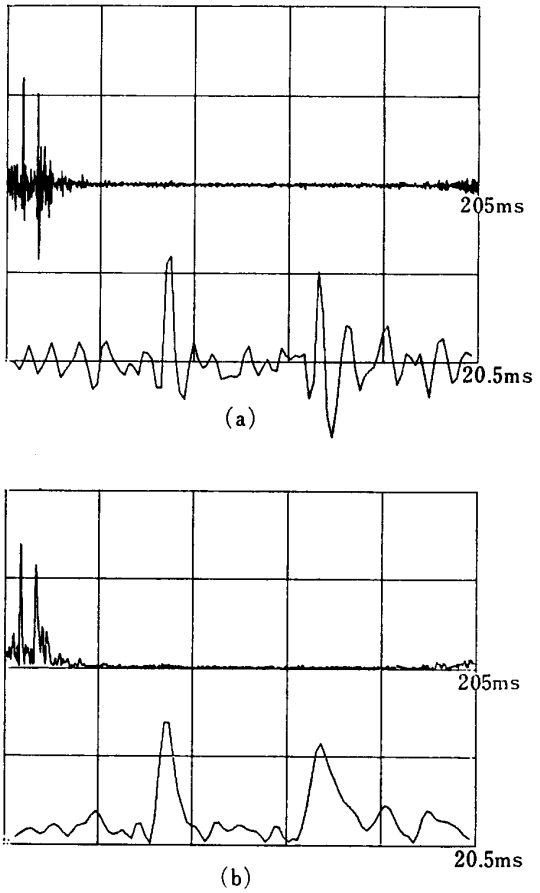

FIG. 9. (a) The inverse Fourier transform of the transfer function. The scales are the same as Fig. 7.
(b) The envelope of (a).

are oscillating very much compared with sound signals in example (1), which is caused probably by the presence of reflected waves (time delayed signals).

The envelope of the inverse Fourier transform of $\boldsymbol{E}[X^* \cdot Y]$ is shown in Fig. 11 in full range and magnified form. It is impossible to find correlation peak from this figure, which is not surprising considering dispersive nature of the flexural wave. So it is essential to use small part of $\boldsymbol{E}[X^* \cdot Y]$. The inverse Fourier transform of $\boldsymbol{E}_{\Delta}[X^* \cdot Y]$ (this is the analogy of $G_{\Delta}(\omega)$) is shown in Fig. 12(a) and its envelope in (b). Frequency range used is from 1750 to 2000 Hz. Two correlation peaks are observed near $\tau = 0$ and two near $\tau = \max$. This is caused by the FFT algorism as explained below.

In the computation of FFT, input signals are regarded as periodic signals with the period $T = N \cdot \Delta t$, where Δt is the sampling period and N is the sampling number. By this periodic nature, correlations obtained by FFT are the mixture of $\phi(\tau)$ and $\phi(T-\tau)$. But in most cases, the correlation becomes zero as $|\tau|$ becomes large, so in $o \leqq \tau \leqq \tau_0$, where τ_0 is much smaller than T, obtained correlation is almost equal to the true correlation and in $T-\tau_0 \leqq \tau \leqq T$, $\phi_{\mathrm{FFT}}(T-\tau) = \phi_{\mathrm{TRUE}}(-\tau)$. If perfect separation is desired, last half of the input signals should be made constantly zero [4].

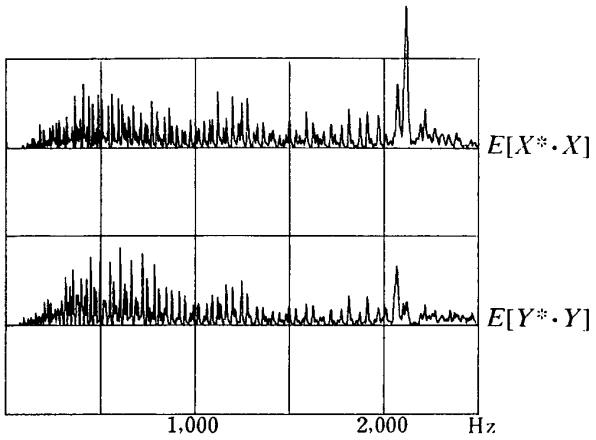

FIG. 10. The power spectra of the flexural vibration of the steel strip excited by tapping.

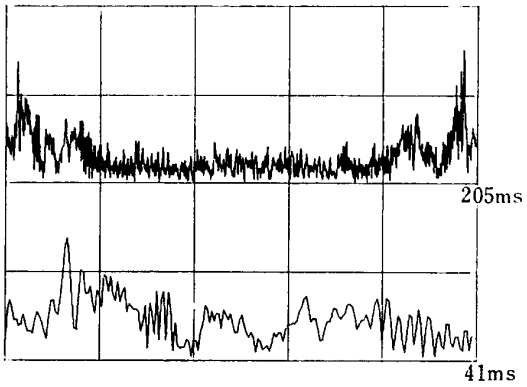

FIG. 11. The envelope of the inverse Fourier transform of $E[X^* \cdot Y]$ of the flexural wave propagation. The full scale of the upper curve is 205 ms and that of the lower is 41 ms.

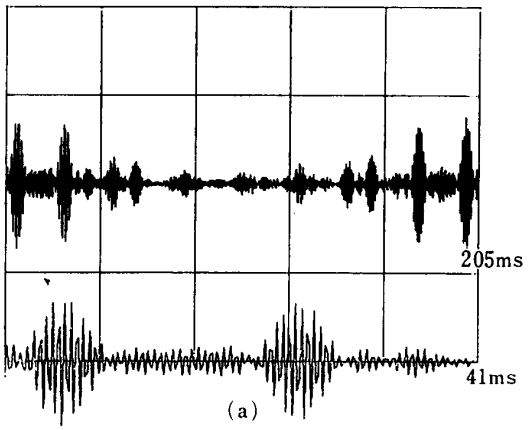

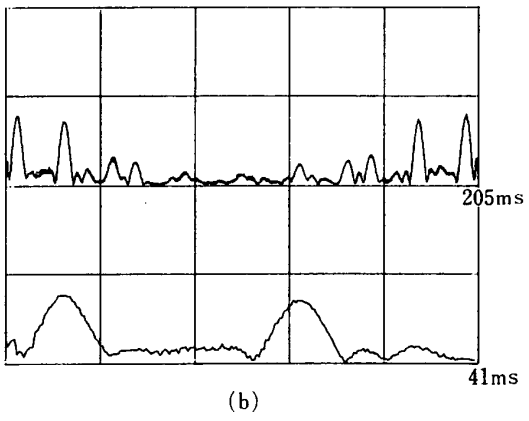

FIG. 12. (a) The inverse Fourier transform of $E_{\Delta}[X^* \cdot Y]$ which is identical with $E[X^* \cdot Y]$ in 1750–2000 Hz while in other frequency range constantly zero. The right side peaks of the upper figure are due to the cyclic nature of FFT and correspond to the peaks at $\tau < 0$.
(b) The envelope of (a).

Now four peaks of Fig. 12 can be explained as follows. The first one is caused by the wave going right direction passing first p.u. 1 and then p.u. 2 as shown in Fig. 13. The second peak is caused by the wave passing p.u. 1 and go to the right

end and reflected back to p.u. 2 with path length of 5 m. The peak near the right end ($\tau=T$) is caused by the wave going left direction. The second peak from the right is caused by the wave going left direction, passing p.u. 2 first, then reflected at the left end and go to p.u. 1 again.

$E_{\Delta}[X^*\cdot Y]$ used to compute Fig. 12 is band limited to 1750–2000 Hz. $E_{\Delta}[X^*\cdot Y]$ is then shifted to 0–250 Hz and inverse Fourier transformed. The results are shown in Fig. 14. The correlation curve Fig. 14(a) changes but its envelope (b) is the same as the envelope of the unshifted correlation Fig. 12(b). This means we can shift $E_{\Delta}[X^*\cdot Y]$ arbitrary on the ω-axis without any change of the correlation envelope, as proved in article 2.

In Fig. 15, correlation envelopes of 8 frequency bands are illustrated. The frequency dependence of the flexural wave velocity is clearly observed.

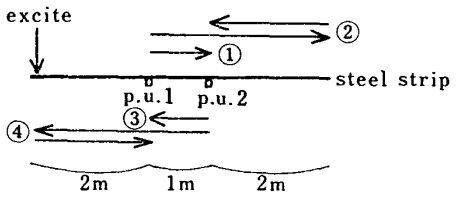

FIG. 13. The flexural wave propagation along a steel strip.

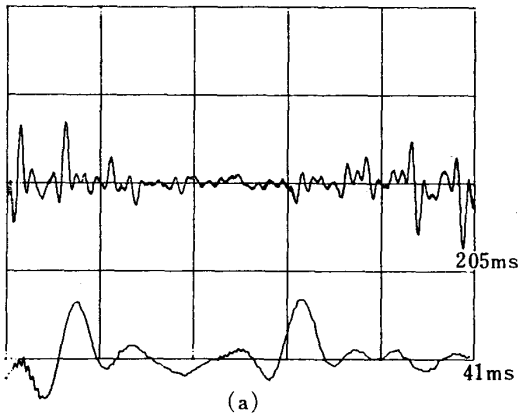

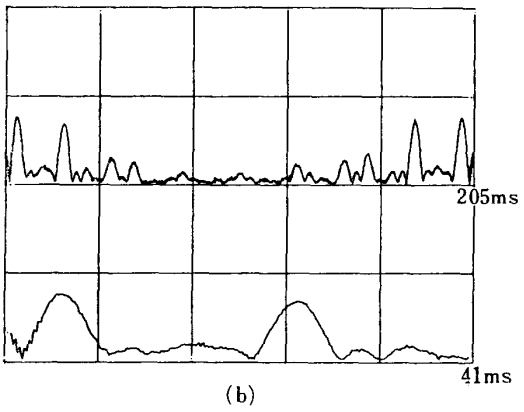

FIG. 14. The inverse Fourier transform of the shifted $E_{\Delta}[X^*\cdot Y]$ and its envelope. The power spectrum of $E_{\Delta}[X^*\cdot Y]$ is shifted on the ω-axis from 1750–2000 Hz to 0–250 Hz.
(a) differs much from Fig. 12(a) but its envelope
(b) is the same as Fig. 12(b).

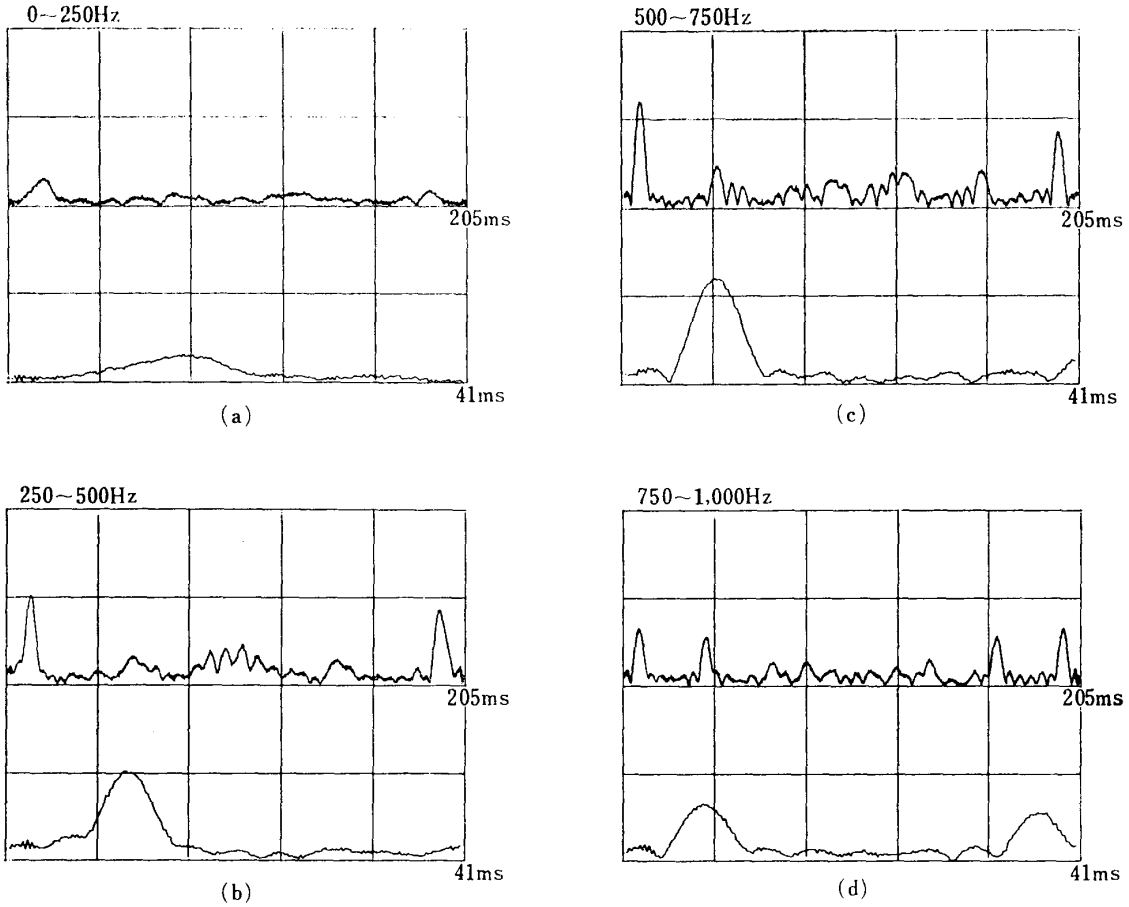

4. Conclusion

An envelope of an arbitrary wave form is shown to be calculated easily by using Fourier transform. This is applied to derive an envelope of a correlation function from a cross-spectrum. And it is discussed that instead of a cross-spectrum, a transfer function can be used advantageously.

The whole signal processing procedure is shown in Fig. 2. Advantages of this method are:

(1) In a measurement of wave propagation, it is common to get oscillating correlation curve. The delay time corresponding to the wave propagation should be obtained from the peak of the correlation envelope, not from the correlation itself. By this new method the correlation envelope is obtained directly.

(2) The influence of the spectral shape of the input signal is eliminated by the use of transfer function. This makes it possible to use sound of clapping hands or striking by hammer as a test signal.

(3) The frequency band to be analysed is easily selected, for it is only a change of computer program. This is especially advantageous to measure dispersive wave as a function of frequency.

The experiments show that this method is useful in measuring noise and vibration propagation.

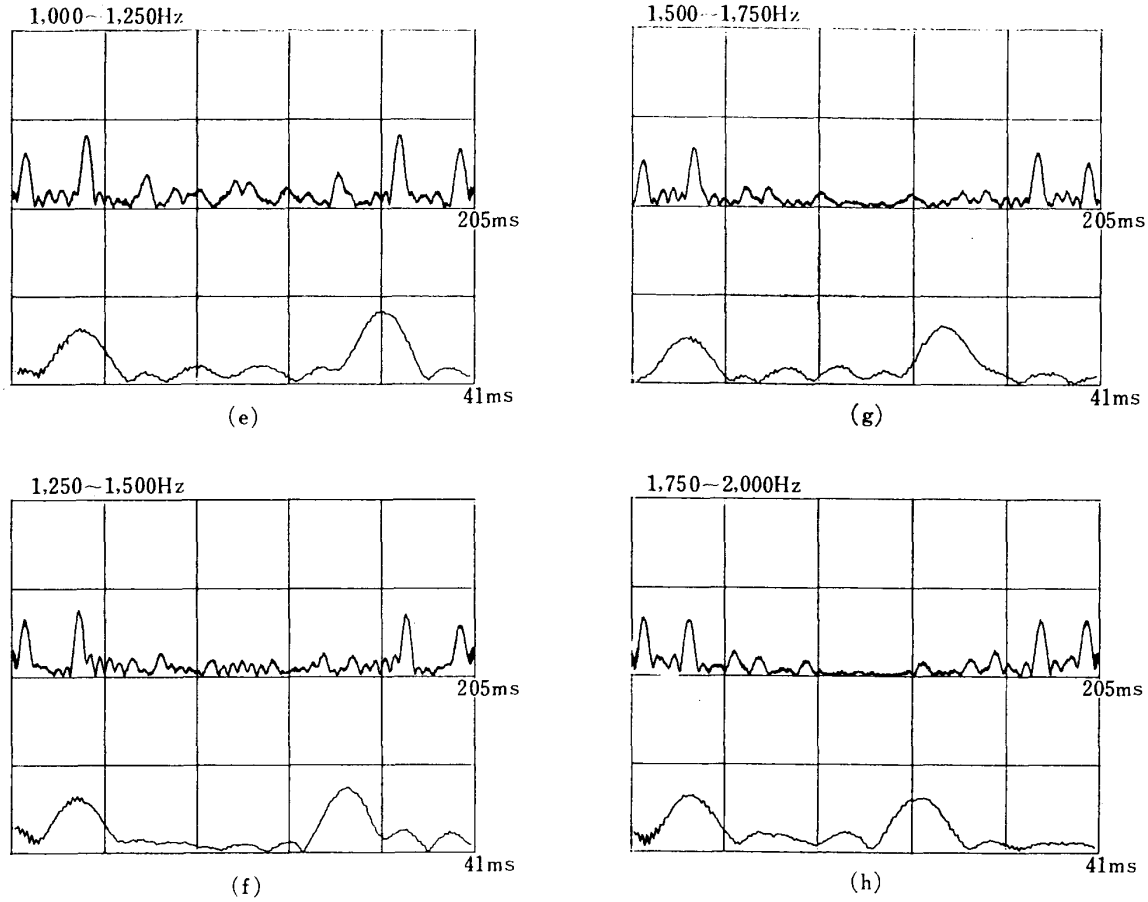

FIG. 15. The envelopes of the inverse Fourier transform of $E_J[X^* \cdot Y]$ varying frequency range with 250 Hz step from 0 to 2000 Hz.

The auther wishes to thank Mr. Ichiro Yamada for his help in computer programming. He also thanks to Sakkokai Foundation for the financial aid.

Department of Instruments and Electronics
Institute of Space and Aeronautical Science
University of Tokyo
June 20, 1974

REFERENCES

[1] P. H. White: Cross Correlation in Structural Systems: Dispersive and Nondispersive Wave, The Journal of the Acoustical Society of America, Vol. 45, No. 5, pp. 1118–1128, 1969.

[2] J. Dugundji: Envelopes and Pre-envelopes of Real Waveforms, IRE Transactions on Information Theory, Vol. IT-4, pp. 53–57, March 1958.

[3] N. Aoshima: Measurement of the Wave Propagation by Correlation Techniques, Report of the Institute of Space and Aeronautical Science, University of Tokyo, No. 447, March 1970.

[4] H. Takahashi: Survey on Fourier Transform, Journal of the Society of Instrument and Control Engineers (Keisoku to Seigyo), Vol. 13, No. 3, pp. 246–253, March 1974. (in Japanese)